Neurobiology of Disease

Inhibitory Interneuron Progenitor Transplantation Restores Normal Learning and Memory in ApoE4 Knock-In Mice without or with Aβ Accumulation

Leslie M. Tong,[1,2] Biljana Djukic,[1,3] Christine Arnold,[3,4,5] Anna K. Gillespie,[1,2] Seo Yeon Yoon,[1] Max M. Wang,[1] Olivia Zhang,[1] Johanna Knoferle,[1,3] John L.R. Rubenstein,[4] Arturo Alvarez-Buylla,[3,5,7] and Yadong Huang[1,2,3,6]

[1]Gladstone Institute of Neurological Disease, San Francisco, California 94158, [2]Biomedical Sciences Graduate Program, Departments of [3]Neurology, [4]Psychiatry, [5]Neurological Surgery, and [6]Pathology, and [7]The Eli and Edythe Broad Center of Regeneration Medicine and Stem Cell Research, University of California, San Francisco, San Francisco, California 94143

Excitatory and inhibitory balance of neuronal network activity is essential for normal brain function and may be of particular importance to memory. Apolipoprotein (apo) E4 and amyloid-β (Aβ) peptides, two major players in Alzheimer's disease (AD), cause inhibitory interneuron impairments and aberrant neuronal activity in the hippocampal dentate gyrus in AD-related mouse models and humans, leading to learning and memory deficits. To determine whether replacing the lost or impaired interneurons rescues neuronal signaling and behavioral deficits, we transplanted embryonic interneuron progenitors into the hippocampal hilus of aged apoE4 knock-in mice without or with Aβ accumulation. In both conditions, the transplanted cells developed into mature interneurons, functionally integrated into the hippocampal circuitry, and restored normal learning and memory. Thus, restricted hilar transplantation of inhibitory interneurons restores normal cognitive function in two widely used AD-related mouse models, highlighting the importance of interneuron impairments in AD pathogenesis and the potential of cell replacement therapy for AD. More broadly, it demonstrates that excitatory and inhibitory balance are crucial for learning and memory, and suggests an avenue for investigating the processes of learning and memory and their alterations in healthy aging and diseases.

Key words: **Alzheimer's disease; apoE; apoE knock-in mice; cell transplantation; learning and memory; MGE-derived GABAergic progenitor**

Introduction

Normal learning and memory are shaped by a balance of excitatory and inhibitory neuronal network activity (Cui et al., 2008; Morellini et al., 2010; Andrews-Zwilling et al., 2012). Aging-related memory deficits, which are exaggerated in individuals with Alzheimer's disease (AD), may result from excitatory–inhibitory imbalance of the hippocampal dentate gyrus due to inhibitory interneuron dysfunction or loss (Palop and Mucke, 2010; Huang and Mucke, 2012). Mutations in amyloid precursor protein (APP), presenilin (PS)-1, or PS-2 cause early-onset autosomal-dominant AD through altered the production of various amyloid-β (Aβ) peptides (Bertram et al., 2010), which account for <1% of AD cases (Campion et al., 1999). Most AD cases are late onset, for which apolipoprotein (apo) E4 is the strongest genetic risk factor; apoE4 carriers make up 60–75% of AD patients (Huang and Mucke, 2012). The expression of apoE4 in humans causes hippocampal hyperactivity (Filippini et al., 2009), and in mice leads to an age- and sex-dependent (female > male) decrease in hilar GABAergic interneurons that correlates with the severity of learning and memory deficits (Li et al., 2009; Andrews-Zwilling et al., 2010; Leung et al., 2012). Similarly, Aβ overproduction or accumulation impairs interneuron function, leading to aberrant dentate gyrus activity and cognitive deficits (Palop et al., 2007; Verret et al., 2012). Patients with mild cognitive impairment (Yassa et al., 2010; Bakker et al., 2012) as well as young, presymptomatic apoE4 carriers (Filippini et al., 2009) display hippocampal hyperactivity. Thus, improving network balance may be effective for preventing or treating cognitive decline in various disease states to promote healthy aging.

Cortical GABAergic interneurons are produced in the embryonic medial ganglionic eminence (MGE; Anderson et al., 1999; Tricoire et al., 2011). Mouse MGE-derived progenitors and immature interneurons grafted into the neonatal and adult CNS migrate, mature, and functionally integrate to modulate the local circuitry (Wichterle et al., 1999; Alvarez-Dolado et al., 2006;

Received Feb. 18, 2014; revised April 29, 2014; accepted June 2, 2014.

Author contributions: L.M.T., B.D., J.L.R.R., A.A.-B., and Y.H. designed research; L.M.T., B.D., C.A., A.K.G., S.Y.Y., M.M.W., O.Z., J.K., and Y.H. performed research; J.L.R.R. and A.A.-B. contributed unpublished reagents/analytic tools; L.M.T., B.D., O.Z., and Y.H. analyzed data; L.M.T., B.D., and Y.H. wrote the paper.

This work was supported in part by Grant RN2-00952 from the California Institute for Regenerative Medicine, Grant AG022074 from the National Institutes of Health, the S.D. Bechtel, Jr. Foundation, the Roddenberry Foundation, and the Hellman Foundation. We thank Laura Leung, Gui-Qiu Yu, Mercedes Paredes, and Derek Southwell for technical advice; Ravikumar Ponnusamy and Iris Lo for assistance on behavioral tests; Diane Nathaniel for electrophysiological data analysis support; Teodoro Meneses for animal husbandry; and Gary Howard, Laura Leung, and Philip Nova for editorial assistance.

Correspondence should be addressed to Dr. Yadong Huang, Gladstone Institute of Neurological Disease, University of California, San Francisco, San Francisco, CA 94158. E-mail: yhuang@gladstone.ucsf.edu.

DOI:10.1523/JNEUROSCI.0693-14.2014

 0270-6474/14/349506-10$15.00/0

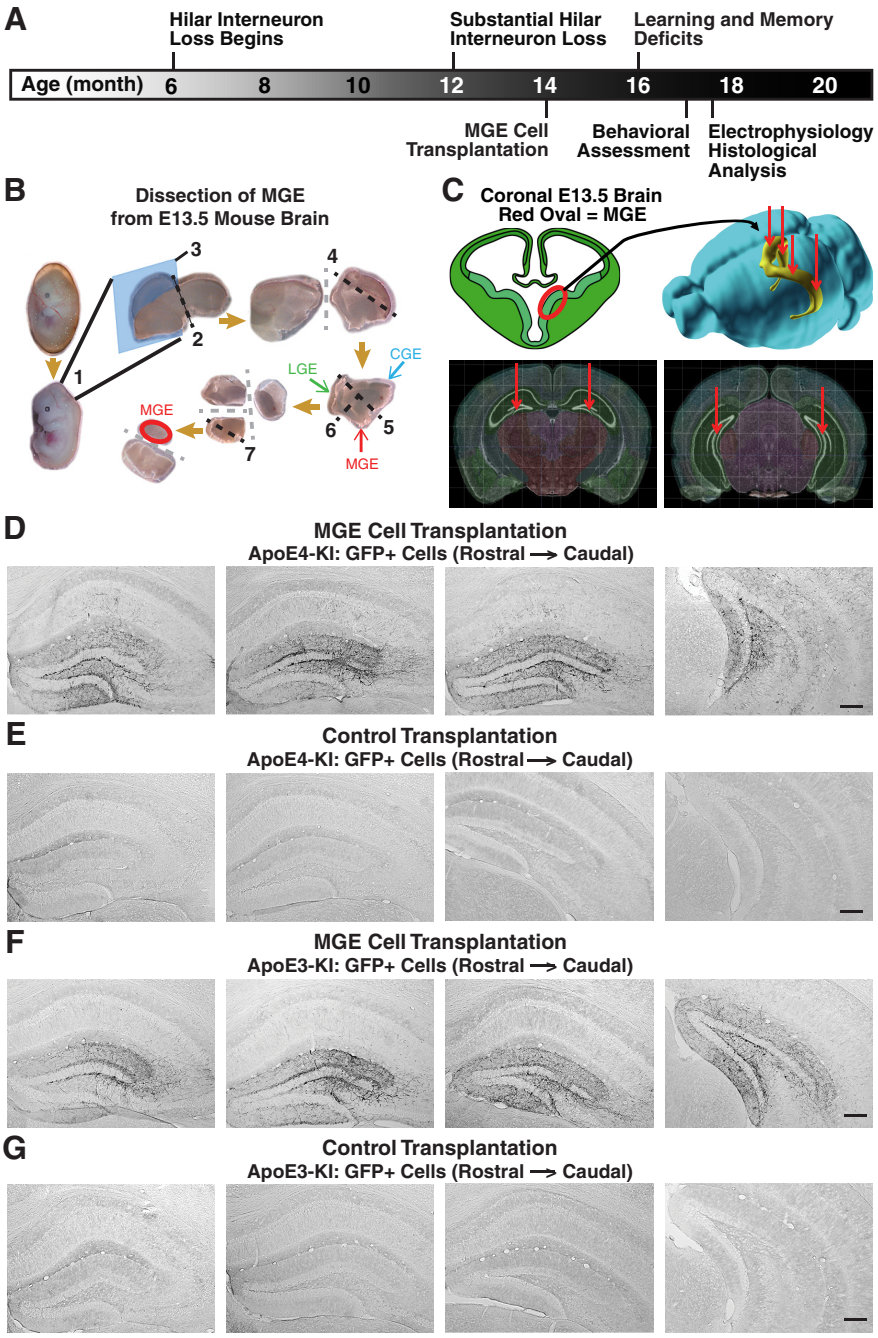

Figure 1. Experimental timeline and protocol, hilar targeting, and migration of transplanted MGE cells in apoE4-KI and apoE3-KI mice. ***A***, Experimental timeline for hilar MGE cell transplantation and evaluation. ***B***, Dissection protocol of MGE from GFP+ E13.5 mouse embryos. (1) Removal of embryonic brain, (2) isolation of the telencephalon by removing hindbrain, (3) sagittal cut to separate two hemispheres, (4) isolation of ventral telencephalon by removing dorsal cortex, (5) removal of caudal ganglionic eminence (CGE) and (6) lateral ganglionic eminence (LGE), and (7) removal of the mantle zone and preoptic area for dorsal MGE collection. ***C***, The dissected MGE cells from GFP+ E13.5 mouse embryos were bilaterally transplanted into the rostral and caudal hilus of 14-month-old apoE4-KI mice. ***D–G***, Immunostaining of GFP+ cells in hippocampal sections 1.2 mm apart from living MGE cell-transplanted apoE4-KI mice (***D***), control-transplanted apoE4-KI mice (***E***), living MGE cell-transplanted apoE3-KI mice (***F***), and control-transplanted apoE3-KI mice (***G***) at 80–90 DAT. Scale bars: ***D–G***, 250 μm.

Southwell et al., 2010; Alvarez Dolado and Broccoli, 2011; Tanaka et al., 2011; Bráz et al., 2012). Some of these transplanted cells survive and remain functional for the life of the host animal (Alvarez-Dolado et al., 2006; Calcagnotto et al., 2010). Importantly, the grafted inhibitory interneurons ameliorate the excitatory–inhibitory imbalance in animal models of neurological disorders, such as epilepsy (Baraban et al., 2009; Martínez-Cerdeño et al., 2010; Zipancic et al., 2010; Alvarez Dolado and Broccoli, 2011; Hunt et al., 2013). Here we demonstrate that transplantation of mouse MGE-derived inhibitory interneuron progenitors into the hippocampal hilus is sufficient to restore normal learning and memory in aged apoE4 knock-in (KI) mice and apoE4-KI mice expressing human APP (hAPP) with familial AD (FAD)-causing mutations (apoE4-KI/hAPP$_{FAD}$).

Materials and Methods

Animals. All protocols and procedures followed the guidelines of the Laboratory Animal Resource Center at the University of California, San Francisco (UCSF). Experimental and control animals had identical housing conditions from birth through sacrifice (12 h light/dark cycle, housed 5 animals/cage, PicoLab Rodent Diet 20). All mouse lines were maintained on a C57BL/6J background strain. ApoE3-KI and apoE4-KI homozygous mouse lines (Taconic; Hamanaka et al., 2000) were born and aged under normal conditions at the Gladstone Institute/UCSF animal facility. apoE4-KI/hAPP$_{FAD}$ mice were generated by crossing apoE4-floxed-KI mice (Bien-Ly et al., 2012) to hAPP$_{FAD}$ mice (J20line; Mucke et al., 2000; Palop et al., 2007; Verret et al., 2012) harboring Swedish (K670N,M671L) and Indiana (V717F) mutations.

Tissue dissection. Donor MGE cells, also on C57BL/6J background strain, were generated by breeding male transgenic β-actin promoter-driven eGFP mice (strain 6567, Jackson Laboratory) with wild-type females. Embryonic day 0.5 (E0.5) was defined as the time when the sperm plug was detected. Embryonic MGE cells were dissected at E13.5 in Leibovitz L-15 medium containing 100 μg/ml DNAseI (Roche), dissociated by pipetting into a single-cell suspension, and collected by centrifugation (3000 $\times$ *g* for 3 min; Wichterle et al., 1999; Alvarez-Dolado et al., 2006; Martínez-Cerdeño et al., 2010; Southwell et al., 2010; Alvarez Dolado and Broccoli, 2011; Hunt et al., 2013). To dissect MGE from green fluorescent protein-positive (GFP+) E13.5 mouse embryos, the embryonic brain was first removed and the telencephalon isolated by removing the hindbrain. A sagittal cut separated the two hemispheres, and the ventral telencephalon was exposed by tearing away the dorsal cortex. The MGE was isolated by removal of caudal and lateral ganglionic eminences, and the dorsal MGE was collected after removing the mantle zone and preoptic area (Fig. 1*B*).

Cell transplantation. Female apoE4-KI and apoE3-KI mice at 14 months of age and apoE4-KI/hAPP$_{FAD}$ mice at 10 months of age were anesthetized with 80 μl of ketamine (10 mg/ml) and xylazine (5 mg/ml) in saline solution and maintained on 0.8–1.0% isoflurane (Henry Schein). Concentrated GFP+ MGE cell suspensions (~600 cells/nl) were loaded into ~60 μm tip diameter, 30° beveled glass micropipette needles (Nanoject, Drummond Scientific Company). Bilateral rostral and caudal stereotaxic sites were drilled with a 0.5 mm microburr (Foredom, Fine Science Tools), and the coordinates used for

hilar transplantation were $X = \pm 1.65$, $Y = 2.00$, $Z = 1.7$ and $X = \pm 2.90$, $Y = 3.20$, $Z = 2.2$, with Z measured from the surface of the brain (David Kopf Instruments). At each transplantation site, ~34 nl (~20,000 cells) were injected and allowed to diffuse for 3 min. For recovery, mice were sutured with 6–0 monofilament nonabsorbent nylon sutures (Ethicon), administered analgesics ketophen (100 μl at 1 mg/ml) and buprenorphine (100 μl at 7.5 μg/ml) in saline solution, and monitored on a heating pad. Control transplant mice received an equivalent volume of heat-shocked dead MGE cells, which were generated by four alternating cycles of 3 min at 55°C and 3 min in dry ice before centrifugation collection (Alvarez-Dolado et al., 2006; Baraban et al., 2009; Southwell et al., 2010).

Behavioral tests. Behavioral tests were performed for MGE cell-transplanted and control-transplanted mice at 70–80 d after transplantation (DAT). All mice were singly housed during behavioral tests. The Morris water maze (MWM) test was conducted in a pool (122 cm in diameter) with room temperature water (22–23°C) with a 10 cm^2 platform submerged 1.5 cm below the surface of opaque water during hidden trials (Andrews-Zwilling et al., 2010; Leung et al., 2012). Mice were trained to locate the hidden platform over four trials per day on hidden platform days 1–5 (HD1–5), where HD0 was the first trial on the first day, with a maximum of 60 s per trial. Each memory trial was conducted for 60 s in the absence of the platform at 24, 72, and 120 h after the final learning session. Memory was assessed as the percentage of time spent in the target quadrant that contained the platform during the learning trials compared with the average percentage of time spent in the nontarget quadrants. For visible trials, a black and white-striped mast (15 cm high) marked the platform location. The platform location and room arrangement remained constant throughout the assay with the exception of moving the platform during the visible trials. Speed was calculated by distance traveled divided by trial duration. Performance was objectively monitored using EthoVision video-tracking software (Noldus Informa-

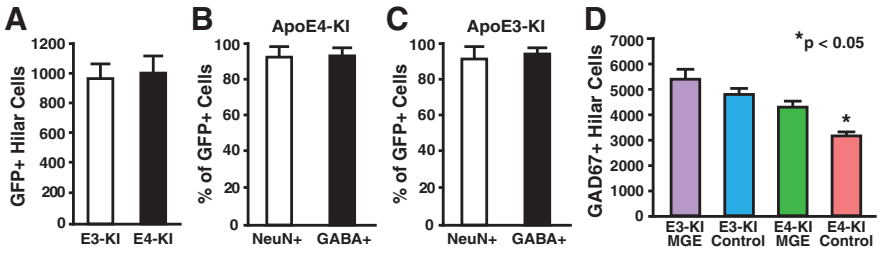

Figure 2. Quantification of GFP+ and total hilar GABAergic interneurons in MGE cell-transplanted apoE4-KI and apoE3-KI mice at 80–90 DAT. ***A***, Quantification of total GFP+ cells in the hilus ($n = 9$–12 sections per brain, 11–13 mice per group). ***B***, ***C***, Quantification of GFP+ cells that were also positive for the mature neuronal marker NeuN and inhibitory neurotransmitter GABA in apoE4-KI (***B***) and apoE3-KI (***C***) mice ($n = 5$–8 sections per brain, 3–5 mice per group). ***D***, MGE cell transplantation significantly increased the total number of GAD67+ cells in the hilus of apoE4-KI mice ($n = 9$–12 sections per brain, 11–13 mice per group). Values are shown as the mean ± SEM. *$p < 0.05$ versus other groups (one-way ANOVA).

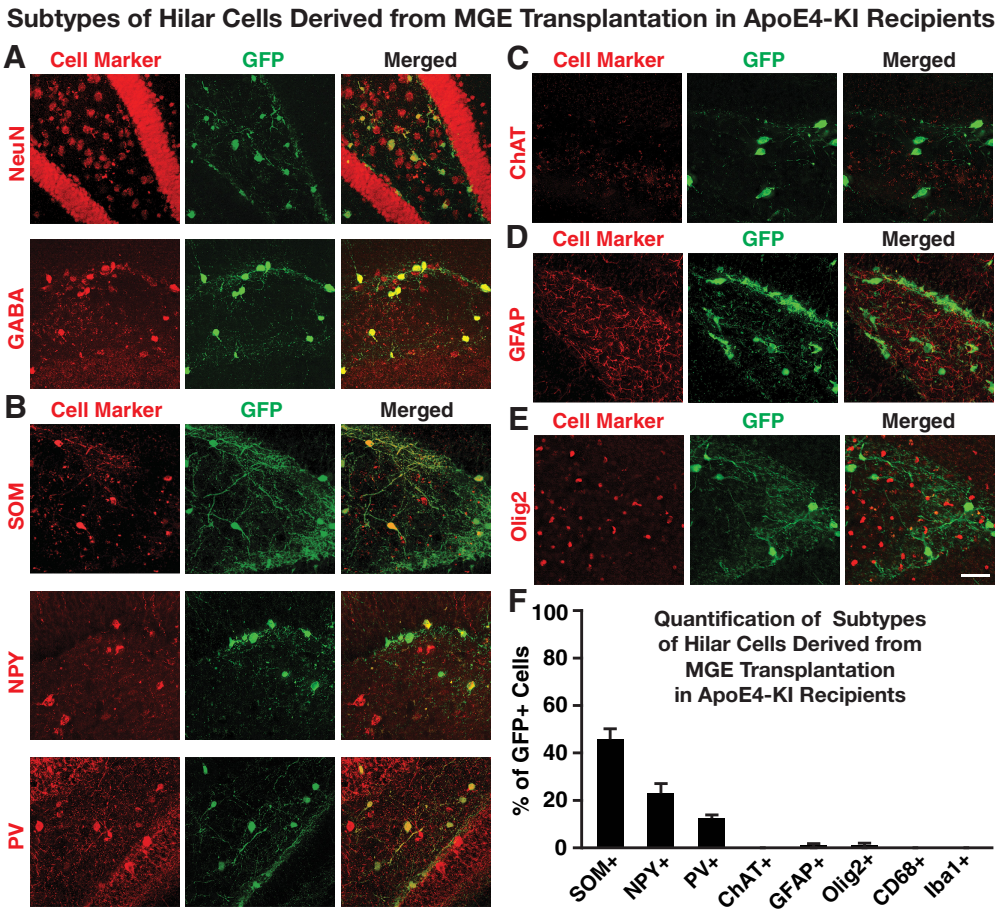

Figure 3. Immunofluorescent analyses of neuronal subtypes derived from transplanted MGE cells in the hippocampal hilus of apoE4-KI mice at 80–90 DAT. ***A***, Transplanted MGE cells were stained positive for NeuN and GABA. ***B***, Immunofluorescent costaining of inhibitory interneuron subtypes positive for SOM, NPY, and PV. ***C–E***, Immunostaining of cells that were positive for ChAT (***C***), GFAP (***D***), or Olig2 (***E***). ***F***, Quantification of the percentage of GFP+ cells that were also positive for different cell markers ($n = 5$–8 sections per brain, 3–5 mice per group for each cell marker). Values are shown as the mean ± SEM. Scale bar, 50 μm.

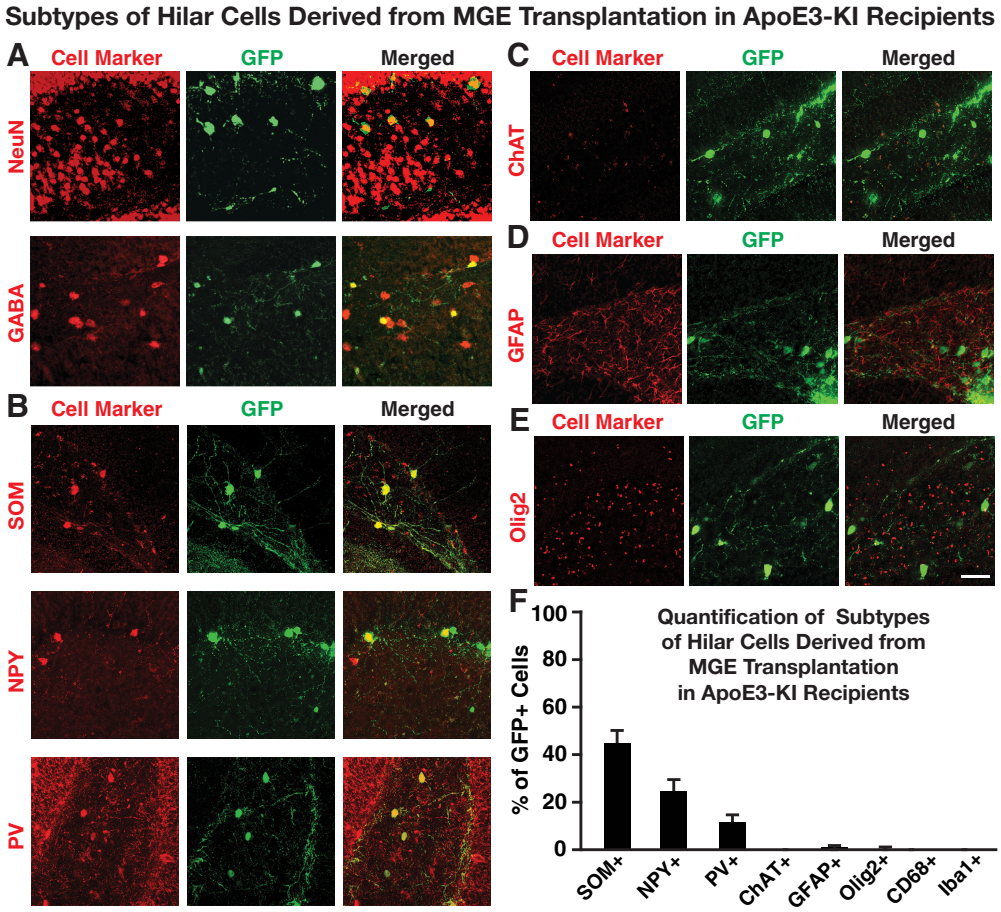

Figure 4. Immunofluorescent analyses of neuronal subtypes derived from transplanted MGE cells in the hippocampal hilus of apoE3-KI mice at 80–90 DAT. ***A***, Transplanted MGE cells were stained positive for NeuN and GABA. ***B***, Immunofluorescent costaining of inhibitory interneuron subtypes positive for SOM, NPY, and PV. ***C–E***, Immunostaining of cells that were positive for ChAT (***C***), GFAP (***D***), or Olig2 (***E***). ***F***, Quantification of the percentage of GFP+ cells that were also positive for different cell markers ($n = 5–8$ sections per brain, 3–5 mice per group for each cell marker). Values are shown as the mean ± SEM. Scale bar, 50 μm.

tion Technology). The open field test assesses habituation and general activity behavior by allowing the mice to explore a new, but empty, environment (Andrews-Zwilling et al., 2012). After at least 2 h of room habituation, mice were placed in an odor-standardized chamber cleaned with 30% EtOH for 15 min. Activity behavior was monitored and analyzed by software from San Diego Instruments. The elevated plus maze evaluates anxiety and exploratory behavior by allowing mice to explore an open, illuminated area (open arm) or hide in a dark, enclosed space (closed arm; Bien-Ly et al., 2011). Here, mice were placed in an odor-standardized maze cleaned with 30% EtOH for 10 min after at least 2 h of room habituation. Behavior was analyzed by infrared photo cells interfacing with Motor Monitor software (Kinder Scientific).

Hippocampal slice preparation and electrophysiology. Acute coronal brain slices (350 μm) were prepared from MGE cell-transplanted and control-transplanted mice 80–90 DAT at 12 or 17 months of age. The modified protective slicing and recovery method of Zhao et al. (2011) was used to improve the health of the slices from aged animals (Zhao et al., 2011). Mice were deeply anesthetized with isoflurane and transcardially perfused with 30 ml of chilled oxygenated (95% O_2, 5% CO_2) slicing artificial CSF (ACSF; 92 mM *N*-methyl-D-glucamine, 2.5 mM KCl, 1.25 mM NaH_2PO_4, 30 mM $NaHCO_3$, 20 mM HEPES, 25 mM glucose, 2 mM thiourea, 5 mM Na-ascorbate, 3 mM Na-pyruvate, 12 mM *N*-acetyl-L-cysteine, 0.5 mM $CaCl_2$, and 10 mM $MgSO_4$). Brains were quickly removed, sliced with the HM650V vibration microtome (Thermo Scientific) and incubated in slicing ACSF for 10 min at 35°C, followed by recovery for 1 h at room temperature in recovery ACSF (92 mM NaCl, 2.5 mM KCl, 1.25 mM NaH_2PO_4, 30 mM $NaHCO_3$, 20 mM HEPES, 25 mM glucose, 2 mM thiourea, 5 mM Na-ascorbate, 3 mM Na-pyruvate, 12 mM *N*-acetyl-L-cysteine, 2 mM $CaCl_2$, and 2 mM $MgSO_4$). After the recovery period, slices were transferred to a holding chamber containing room temperature oxygenated recording ACSF (126 mM NaCl, 3 mM KCl, 1.25 mM NaH_2PO_4, 26 mM $NaHCO_3$, 20 mM glucose, 2 mM $CaCl_2$, and 2 mM $MgCl_2$). For recording, slices were placed in the recording chamber of a BX51WI microscope (Olympus) equipped with infrared differential interference contrast optics (900 nm) and epifluorescence, and perfused with warmed (30°C) oxygenated recording ACSF at a rate of 3 ml/min. Whole-cell patch-clamp recordings were obtained from visually identified granule cells and hilar interneurons using borosilicate glass pipettes (4–5 MΩ), a Multiclamp 700B amplifier (Molecular Devices), and WinLTP acquisition software (University of Bristol, Bristol, UK). Recordings were discarded if series resistance (Rs) values were >25 MΩ, or if Rs values varied by >25% during the course of the experiment. All data analyses were performed off-line with Clampfit 10.2 software (Molecular Devices).

Spontaneous EPSCs and IPSCs were recorded in the same cells by voltage-clamping the membrane potential at the reversal potential of the GABAergic current (−50 mV) and glutamatergic current (10 mV), respectively. To stabilize recordings at the depolarizing membrane potential, patch pipettes were filled with an internal solution containing the following: 120 mM $CsMeSO_3$, 0.5 mM EGTA, 10 mM BAPTA, 10 mM HEPES, 2 mM Mg-ATP, 0.3 mM Na-GTP, and 5 mM QX-314. Events were sampled for 200 s and detected with a cutoff of ±5 pA.

Intrinsic excitability of interneurons was assessed by measuring the firing rate in response to a series of depolarizing current injections (1 s; 0.05–1 nA). Patch pipettes were filled with an internal solution containing the following: 100 mM K-gluconate, 20 mM KCl, 10 mM HEPES, 4 mM

Mg-ATP, 0.3 mM Na-GTP, 10 mM phosphocreatine, and 0.2% biocytin. After the experiment, slices were fixed and stained for biocytin, somatostatin, and parvalbumin to confirm the identity of the recorded cells.

Immunohistochemistry. Animals were transcardially perfused with 0.9% (w/v) saline solution then with 4% (w/v) paraformaldehyde (PFA), and whole brains were collected and drop fixed in 4% PFA for 24 h at 4°C. After rinsing in PBS, tissue was cryoprotected in 30% (w/v) sucrose and sectioned coronally (30 μm) with a frozen sliding microtome (Leica) for floating section immunohistochemistry. *Post hoc* electrophysiology slices (vibratome-cut 350-μm-thick slices) were also stained as floating sections. Floating sections were immunostained overnight with the following primary antibodies: rabbit anti-GFP (1:2000; Abcam); goat anti-GFP (1:3000; Abcam); chicken anti-GFP (1:2000; Abcam); biotinylated mouse anti-NeuN (1:300; Abcam); rabbit anti-GABA (1:2500; Sigma); rat anti-somatostatin (1:100; Millipore); goat anti-somatostatin (1:250; Santa Cruz Biotechnology); rabbit anti-NPY (1:6000; Sigma); rabbit anti-parvalbumin (1:1000; Millipore); goat anti-ChAT (1:300; Millipore); rabbit anti-GFAP (1:2000; Dako); rabbit anti-Olig2 (1:300; Millipore); rabbit anti-ionized calcium-binding adapter molecule-1 (Iba1; 1:3000; Wako); rat anti-mouse CD68 (1:300; Serotec); and biotinylated mouse anti-human Aβ 3D6B (1:700; Elan). Secondary antibodies used were as follows: Alexa Fluor 488 donkey anti-goat; Alexa Fluor 488 donkey anti-rabbit; Alexa Fluor 488 goat anti-chicken; Alexa Fluor 594 donkey anti-rabbit; Alexa Fluor 594 donkey anti-goat; Alexa Fluor 594 donkey anti-rat; Alexa Fluor 647 donkey anti-goat (1:2000; Life Technologies); biotinylated goat anti-rabbit (1:200; Vector Laboratories); biotinylated donkey anti-mouse (1:250; Jackson Immunoresearch); and biotinylated rabbit anti-rat (1:250; Vector Laboratories). Alexa Fluor 594 streptavidin was used to detect biotin and biocytin (1:500; Life Technologies). Diaminobenzidine (DAB) immunohistochemistry development was performed using Vectastain ABC amplification kit (Vector Laboratories) and DAB (Sigma) as a chromagen substrate for 1–5 min. There were no tumors observed under gross and histological examinations.

Image collection and cell quantification. Histological images were collected using a Biorevo BZ-9000 Keyence digital microscope, a Leica spinning disk confocal microscope, or a Bio-Rad scanning confocal microscope. Quantification of interneuron subtypes was obtained manually by observations performed on an upright epifluorescent DM500B Leica microscope and on a Keyence digital microscope. Quantification of microglia (markers of Iba1 and CD68) was obtained using the semiautomated Image-based Tool for Counting Nuclei (ITCN) plugin in ImageJ for images covering 0.5 mm^2 of the dentate gyrus. Quantification of GAD67+ and GFP+ cells was conducted on every 10th section (30 μm) across the whole hippocampus using the semiautomated ITCN plugin in ImageJ for captured images.

Aβ analysis. Aβ was immunostained as reported (Bien-Ly et al., 2011, 2012). Hippocampal plaque loads were quantified using the ImageJ Measure tool on manually outlined hippocampal images of Aβ immunostaining. Hippocampal Aβ concentrations were measured by sandwich ELISA with capture antibodies mouse anti-A$\beta_{1\text{-}x}$ 266 (10 μg/ml) and mouse anti-Aβ_{42} 21F12 (5 μg/ml), and detection antibody mouse anti-human Aβ 3D6B (0.5 μg/ml; Bien-Ly et al., 2011, 2012). Development and detection was performed with an HRP-avidin and TMB-ELISA substrate (Thermo Scientific) read on a Spectramax 190 Plate Reader (Molecular Devices).

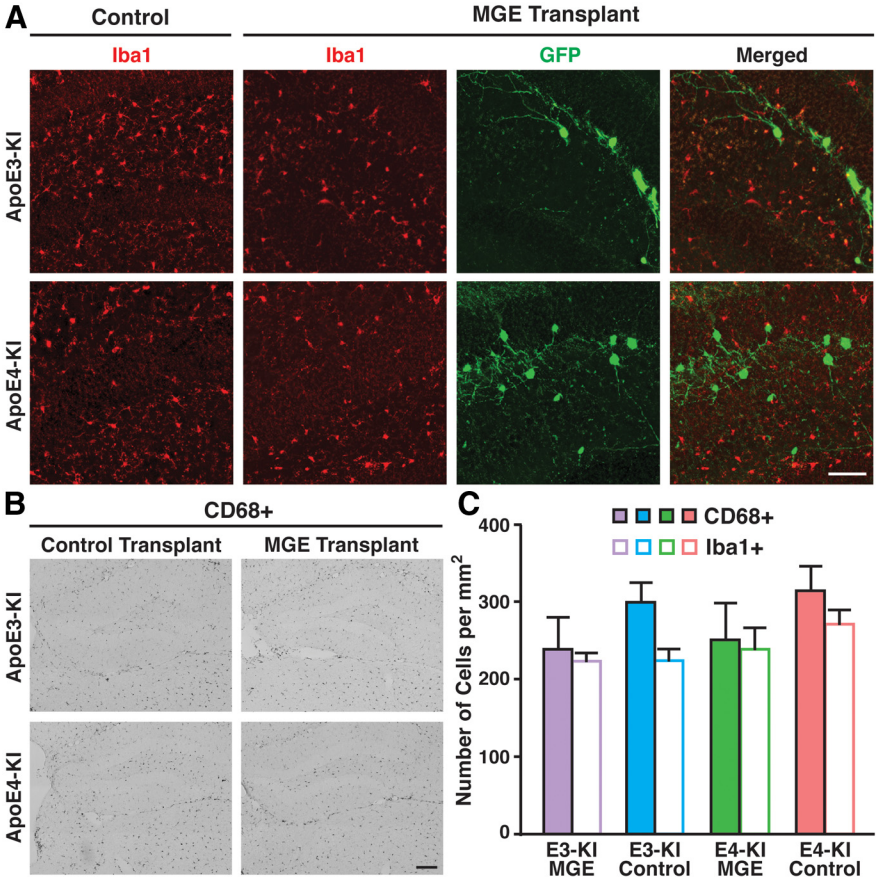

Figure 5. Examination of microglia as a marker for inflammation. ***A***, Immunofluorescent staining of microglial marker Iba1 showed no microglia clustering around the grafted cells. ***B***, Immunostaining of activated microglia marker CD68 showed no significant differences between MGE cell-transplanted and control mice. ***C***, Quantification of CD68+ and Iba1+ cells per square millimeter ($n = 5–8$ sections per brain, 3–5 mice per group). Values are shown as the mean ± SEM. Scale bars: ***A***, 50 μm; ***B***, 250 μm.

Statistical analysis. All statistical analyses for electrophysiology were performed using IGOR Pro software (WaveMetrics), and all other analyses were performed using Prism 6 software (GraphPad). Differences between means were assessed by *t* test, one-way ANOVA, or repeated-measures ANOVA, followed by Bonferroni or Tukey-Kramer *post hoc* tests, as noted in text and figure legends. In all cases, a *p* value of <0.05 was considered to be statistically significant. All error bars represent ±SEM.

Results

Hilar transplantation and survival of MGE-derived GABAergic interneuron progenitors

Freshly dissected MGE cells were transplanted bilaterally into the hilus of 14-month-old female apoE4-KI mice with substantial hilar interneuron loss at rostral and caudal sites (Fig. 1*A–C*; Andrews-Zwilling et al., 2010; Leung et al., 2012). Donor cells were collected from the MGE of E13.5 mouse embryos that express GFP in all cells (Fig. 1*B*,*C*; Alvarez-Dolado et al., 2006; Baraban et al., 2009; Calcagnotto et al., 2010; Southwell et al., 2010; Zipancic et al., 2010; Tanaka et al., 2011; Hunt et al., 2013). Controls included MGE cell-transplanted apoE3-KI mice and control-transplanted apoE3-KI and apoE4-KI mice (Alvarez-Dolado et al., 2006; Baraban et al., 2009; Southwell et al., 2010). The transplanted GFP+ MGE cells survived at least 90 DAT and migrated throughout the hilus, with neurites extending into the

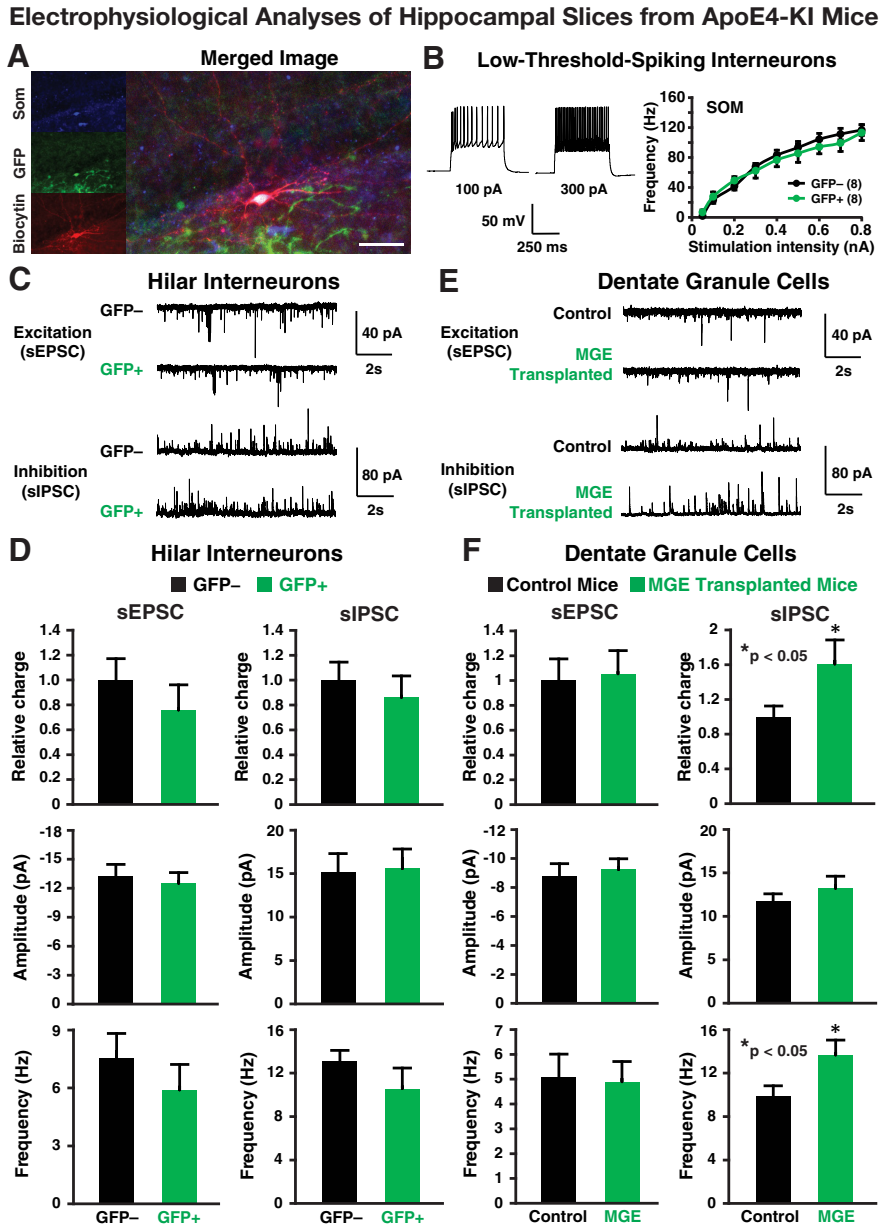

Figure 6. Electrophysiological analyses of transplanted and endogenous cells in acute hippocampal slices from 17-month-old apoE4-KI mice at 80–90 DAT. ***A***, *Post hoc* staining of a low-threshold-spiking GFP+ interneuron filled with biocytin during recording was positive for SOM. Scale bar, 50 μm. ***B***, Representative voltage traces from a GFP+ hilar cell are shown. The intrinsic excitability study (frequency of firing vs stimulation intensity) of GFP+ hilar cells revealed firing properties indistinguishable from endogenous (GFP−) hilar cells. ***C***, ***D***, Transplanted GFP+ cells displayed spontaneous EPSCs (sEPSCs) and spontaneous IPSCs (sIPSCs; ***C***) at frequencies and amplitudes (***D***) comparable to endogenous (GFP−) hilar interneurons. ***E***, ***F***, Current traces (***E***) from dentate granule neurons in control and MGE cell-transplanted apoE4-KI mice show no quantifiable changes (***F***) in sEPSCs, but a significant increase in the frequency of sIPSCs, leading to an overall increase in inhibitory charge transfer. Values are shown as the mean ± SEM. *$p < 0.05$, *t* test. $n = 8$–15 cells per group.

molecular layer of the dentate gyrus in both apoE4-KI (Fig. 1*D*) and apoE3-KI (Fig. 1*F*) mice. No GFP+ cells were found in hippocampi of control-transplanted apoE4-KI and apoE3-KI mice (Fig. 1*E*,*G*). Transplanted MGE cells survived and matured into inhibitory interneurons, as marked by NeuN and GABA, at similar levels in apoE4-KI (94.8 ± 2.3% and 96.1 ± 2.1%, respectively; Figs. 2*A*,*B*, 3*A*) and apoE3-KI (93.6 ± 4.7% and 93.8 ± 3.4%; Figs. 2*A*,*C*, 4*A*) recipients. Importantly, transplantation significantly increased the total number of GAD67+ hilar interneurons in apoE4-KI mice, reaching a level similar to that of control apoE3-KI mice (Fig. 2*D*). Transplanted MGE cells developed predominantly into somatostatin-positive (SOM+) interneurons (E4-KI, 45.7 ± 4.4%; E3-KI, 45.0 ± 5.3%), followed by neuropeptide-Y-positive (NPY+; E4-KI, 23.0 ± 4.1%; E3-KI, 23.8 ± 3.5%) and parvalbumin-positive (PV+) interneurons (E4-KI, 12.5 ± 2.4%; E3-KI, 12.1 ± 2.6%), in apoE4-KI (Fig. 3*B*,*F*) and apoE3-KI (Fig. 4*B*,*F*) mice. There were no significant differences of the GFP+ MGE-derived interneuron subtypes between apoE4-KI and apoE3-KI mice (Figs. 3*F*, 4*F*). Negligible numbers of ChAT+, GFAP+, Olig2+, CD68+, or Iba1+ cells were derived from the transplanted GFP+ MGE cells at 90 DAT (Figs. 3*C–F*, 4*C–F*). No neuroinflammatory response to MGE cell transplantation was detected, as indicated by similar microglia densities in MGE- and control-transplanted mouse hippocampal sections immunostained at 90 DAT for Iba1 and CD68 (Fig. 5).

Functional maturation and integration of transplanted MGE-derived GABAergic interneurons in the hippocampus

Electrophysiological recordings in acute hippocampal slices from 17-month-old mice at 80–90 DAT confirmed functional maturation and integration of transplanted MGE cells. Patch-clamp recordings from most transplanted GFP+ cells (Figs. 6*A*, 7*A*) revealed intrinsic firing properties typical of SOM+ low-threshold spiking interneurons that did not differ significantly from endogenous (GFP−) interneurons in apoE4-KI (Fig. 6*B*) and apoE3-KI (Fig. 7*B*) mice. *Post hoc* staining of these cells filled with biocytin during recording revealed that they were indeed SOM+ interneurons (Fig. 6*A*). The transplanted GFP+ MGE cells displayed spontaneous EPSCs and IPSCs of comparable amplitude and frequency as endogenous hilar interneurons (Figs. 6*C*,*D*, 7*C*,*D*), suggesting their complete integration in the host hippocampal network in both apoE4-KI (Fig. 6*C*,*D*) and apoE3-KI (Fig. 7*C*,*D*) recipients. Most importantly, the dentate granule neurons in MGE cell-transplanted brains showed increased frequency of spontaneous inhibitory currents and increased inhibitory charge transfer relative to control-transplanted brains, indicating that the grafted interneurons functionally modified the hippocampal circuitry (Figs. 6*E*,*F*, 7*E*,*F*).

Transplantation of MGE-derived GABAergic interneurons rescues apoE4-induced cognitive deficits in aged mice

To determine the behavioral effects of MGE cell transplantation, mice were evaluated for cognitive function in the MWM. MGE

cell transplantation restored normal learning in aged apoE4-KI mice at 70–80 DAT, matching the performance of apoE3-KI mice (Fig. 8*A*). MGE cell transplantation also rescued apoE4-induced memory deficits in a probe trial (Fig. 8*B*). No vision or motor deficits were apparent, as determined by visible trials (Fig. 8*A*) and swim speed (Fig. 8*C*). The results of open field and elevated plus maze assays provided additional evidence that MGE cell transplantation corrected the abnormal activity, anxiety, and exploratory behaviors of apoE4-KI mice (Fig. 8*D*,*E*). In all behavioral tests, no significant differences were observed between control- and MGE cell-transplanted apoE3-KI mice (Fig. 8), suggesting that moderately increasing the numbers of hilar inhibitory interneurons in unimpaired brains does not alter learning, memory, or other behaviors.

Transplantation of MGE-derived GABAergic interneurons rescues cognitive deficits in the presence of Aβ accumulation in apoE4-KI mice

In AD patients, apoE4 is often associated with enhanced brain Aβ accumulation (Huang and Mucke, 2012); Aβ also impairs GABAergic interneurons (Verret et al., 2012). ApoE4-KI mice expressing human APP with FAD-causing mutations (apoE4-KI/hAPP$_{FAD}$) accumulate high levels of Aβ (Bien-Ly et al., 2012) and exhibit severe learning and memory impairments as early as 3 months of age (Palop et al., 2007; Verret et al., 2012). To explore whether MGE cell transplantation rescues learning and memory deficits in the presence of both Aβ accumulation and apoE4, we transplanted MGE cells into the hilus of the dentate gyrus of 10-month-old apoE4-KI/hAPP$_{FAD}$ mice that displayed severe learning and memory deficits (Fig. 9*A*,*B*). Age-matched wild-type mice without transplantation were used as controls. ApoE4-KI mice without hAPP$_{FAD}$ expression, which did not develop learning and memory deficits at 12 months of age (Leung et al., 2012), were also included as controls. Strikingly, MGE cell transplantation completely rescued both learning and memory deficits in apoE4-KI/hAPP$_{FAD}$ mice to levels indistinguishable from wild-type mice when tested 2 months later (Fig. 9*A*,*B*). MGE cell transplantation did not significantly alter hippocampal plaque loads or Aβ levels (Fig. 9*E*–*G*). Histological analysis revealed that transplanted GFP+ MGE cells survived well in the hippocampal circuitry in the presence of Aβ plaque buildup (Fig. 9*C*,*D*). Electrophysiological analyses confirmed that transplanted GFP+ MGE cells functionally integrated in the hippocampal circuitry in the presence of Aβ plaques (Fig. 10).

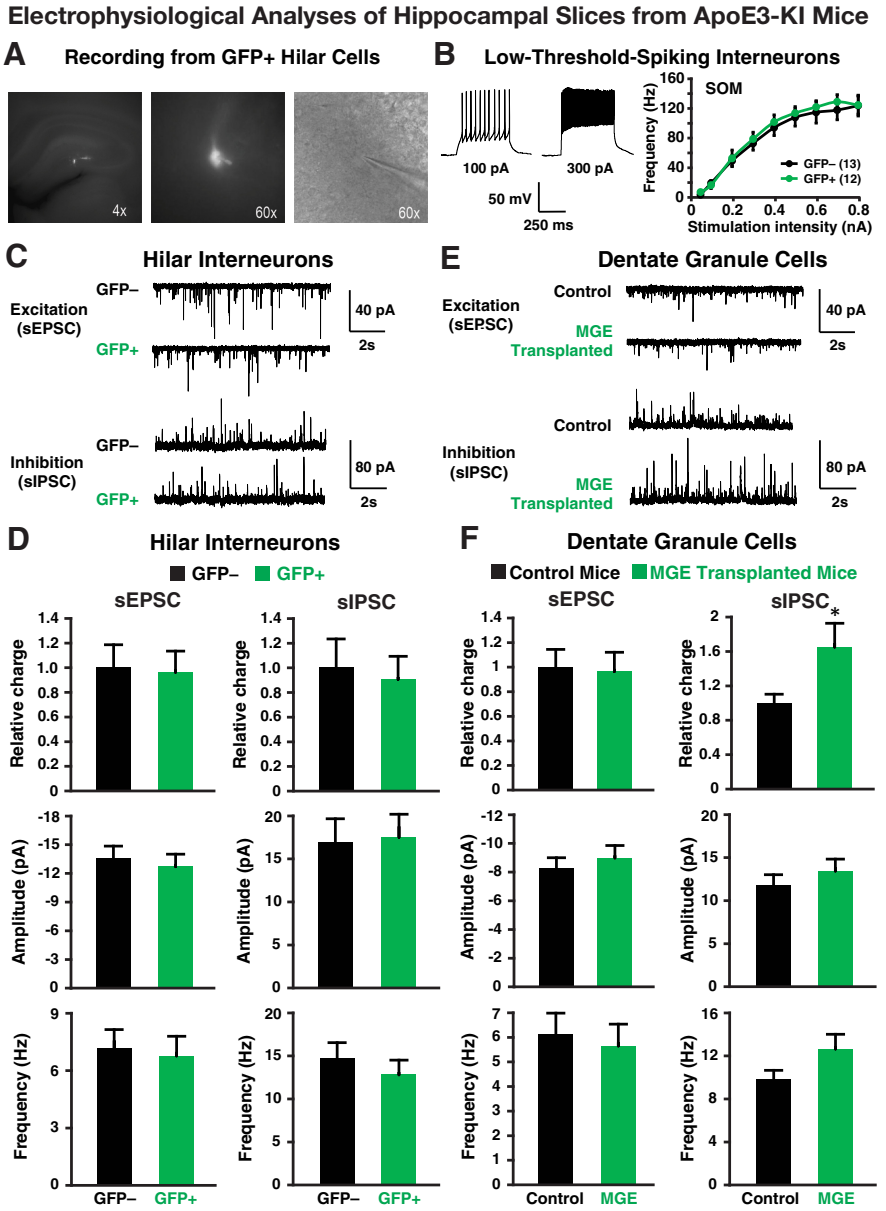

Figure 7. Electrophysiological analyses of transplanted and endogenous cells in acute hippocampal slices from 17-month-old apoE3-KI mice at 80–90 DAT. ***A***, Fluorescent and bright-field images (4× and 60×) of a GFP+ hilar cell during electrophysiological recording. ***B***, Representative voltage traces from a GFP+ hilar cell are shown. The intrinsic excitability study (frequency of firing vs stimulation intensity) of GFP+ hilar cells revealed firing properties indistinguishable from endogenous (GFP−) hilar cells. ***C***, ***D***, Transplanted GFP+ cells received spontaneous EPSCs (sEPSCs) and spontaneous IPSCs (sIPSCs; ***C***) from the host cells at frequencies and amplitudes (***D***) comparable to endogenous hilar interneurons (GFP−). ***E***, ***F***, Current traces (***E***) from dentate granule neurons in control and MGE cell-transplanted apoE3-KI mice reveal no quantifiable changes (***F***) in excitatory input (i.e., sEPSCs), but a significant increase in inhibitory charge transfer. Values are shown as the mean ± SEM. *$p < 0.05$, *t* test. $n = 8$–15 cells per group.

Discussion

We have previously shown that apoE4-KI mice have a significant age-dependent decrease in hilar GABAergic interneurons that correlates with the extent of apoE4-induced learning and memory deficits in aged mice (Li et al., 2009; Andrews-Zwilling et al., 2010; Leung et al., 2012). Similarly, Aβ overproduction or accumulation impairs interneuron function, leading to aberrant dentate gyrus activity, and learning and memory deficits (Palop et al., 2007; Verret et al., 2012). The current study demonstrates that hilar transplantation of MGE-derived inhibitory interneuron progenitors restores normal learning and memory in these two widely used AD-related mouse models—apoE4 expression and

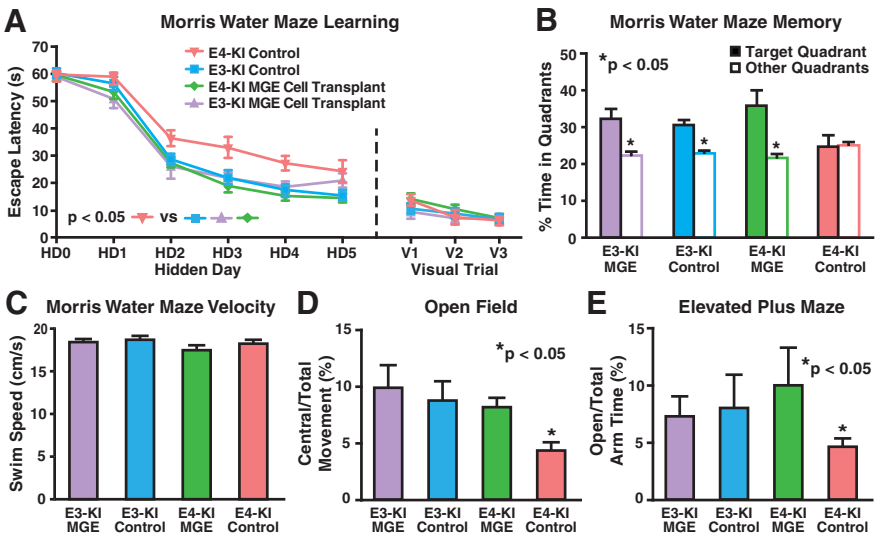

Figure 8. MGE cell transplantation rescued behavioral deficits of 17-month-old apoE4-KI mice at 70–80 DAT. ***A***, MWM test showed a rescue of learning over 5 d of hidden platform trials in MGE cell-transplanted apoE4-KI mice, with no differences in visual trials. Points represent averages of daily trials. V, Visible platform day (two trials per session, two sessions per day). *y*-axis indicates the time to reach the target platform (escape latency, mean ± SEM). ***B***, The probe trial of the MWM test showed a rescue of memory 120 h after the last learning trial in MGE cell-transplanted apoE4-KI mice. ***C***, Swim speeds did not differ significantly among all groups. ***D***, ***E***, MGE cell transplantation ameliorated apoE4-induced behavioral deficits in the open field (***D***) and elevated plus maze (***E***) tests. Values are shown as the mean ± SEM. $*p < 0.05$ repeated-measures ANOVA (***A***), one-way ANOVA (***C***), and *t* test (***B***, ***D***, and ***E***). $n = 9–13$ mice per group.

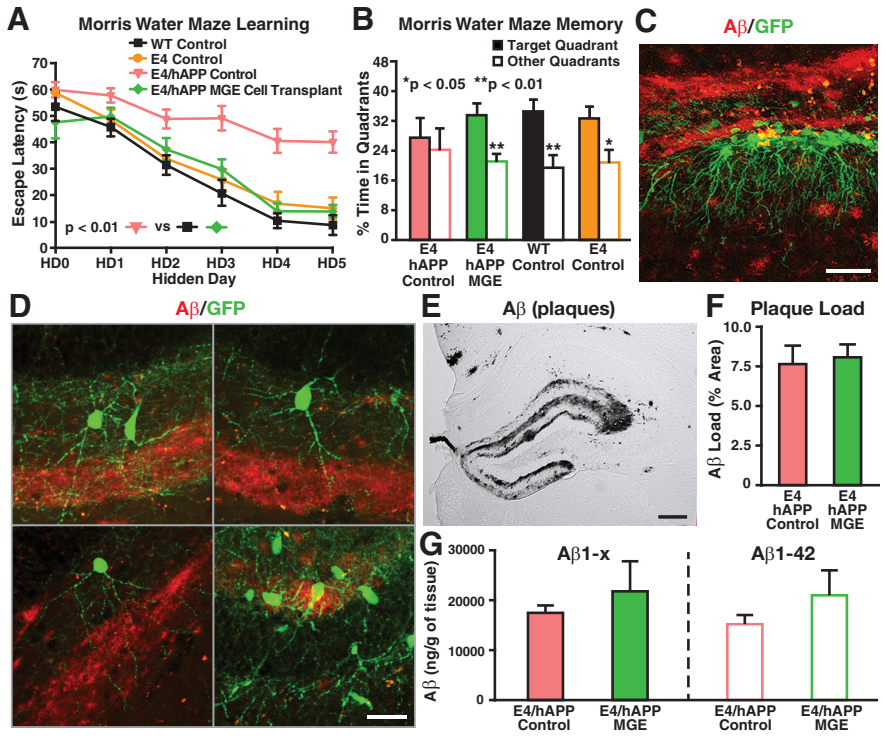

Figure 9. MGE cell transplantation rescued learning and memory deficits of 12-month-old apoE4-KI/hAPP$_{FAD}$ mice at 70–80 DAT. ***A***, ***B***, MWM test of learning (***A***) and memory (***B***) for transplanted and control apoE4-KI/hAPP$_{FAD}$, wild-type, and apoE4-KI mice ($n = 7–12$ mice per group). ***C***, ***D***, Transplanted GFP+ cells survived and integrated in the dentate gyrus in the presence of plaques (***C***), with mature morphologies and processes extending through the plaques (***D***). ***E–G***, DAB immunostaining of hippocampal Aβ (***E***) as well as quantification of plaque load (***F***) and Aβ levels (***G***) showed no significant effects of MGE cell transplantation on Aβ accumulation. $n = 5–8$ sections per brain, 5 mice per group. Values are shown as the mean ± SEM. $**p < 0.01$ repeated-measures ANOVA (***A***) and *t* test (***B***). Scale bars: ***C***, 50 μm; ***D***, 20 μm; ***E***, 250 μm.

Aβ accumulation (Huang and Mucke, 2012). This directly demonstrates the importance of inhibitory interneuron impairments in age-related cognitive decline in mouse models of AD.

Dysfunction of the GABAergic system may also contribute to cognitive impairment in humans. AD patients have decreased GABA and somatostatin levels in the brain and CSF (Davies et al., 1980; Bareggi et al., 1982; Zimmer et al., 1984; Hardy et al., 1987; Seidl et al., 2001), and these alterations were more severe in apoE4 carriers (Grouselle et al., 1998). ApoE4 is associated with increased brain activity at rest and in response to memory tasks (Filippini et al., 2009; Dennis et al., 2010), possibly reflecting impaired GABAergic inhibitory control. Furthermore, GABA levels in human CSF decrease with age (Bareggi et al., 1982)—the strongest risk factor for AD. Thus, aging- and AD-related memory deficits in humans may also result from an excitatory–inhibitory imbalance of the hippocampal dentate gyrus due to inhibitory interneuron dysfunction or loss (Palop and Mucke, 2010; Huang and Mucke, 2012). The current study provides a proof of concept for developing inhibitory interneuron replacement therapies for treatment of AD. In support of this possibility, a recent study (Liu et al., 2013) showed that transplantation of human embryonic stem cell-derived MGE-like cells rescued learning and memory deficits induced by acute hippocampal lesions in mice.

Strikingly, the grafted MGE-derived inhibitory interneurons not only survive and functionally integrate in the hippocampus of aged mice (12–17 months of age) but also do so in an apparently toxic environment—the presence of apoE4 and Aβ accumulation. Since wild-type mouse MGE-derived GABAergic interneuron progenitors, which express wild-type mouse apoE, survive and integrate equally well in the hippocampal hilus of apoE3-KI and apoE4-KI mice for >3 months, this suggests that the detrimental effect of apoE4 on hilar GABAergic interneurons is cell autonomous. The observation that the wild-type mouse MGE cells also survive and integrate well in the hippocampal hilus of apoE4-KI mice with significant Aβ plaque buildup further supports this conclusion. This is important for potential stem cell-based therapy of AD in the future, indicating that transplanted human MGE-like cells without apoE4 expression or Aβ overproduction would have a good chance

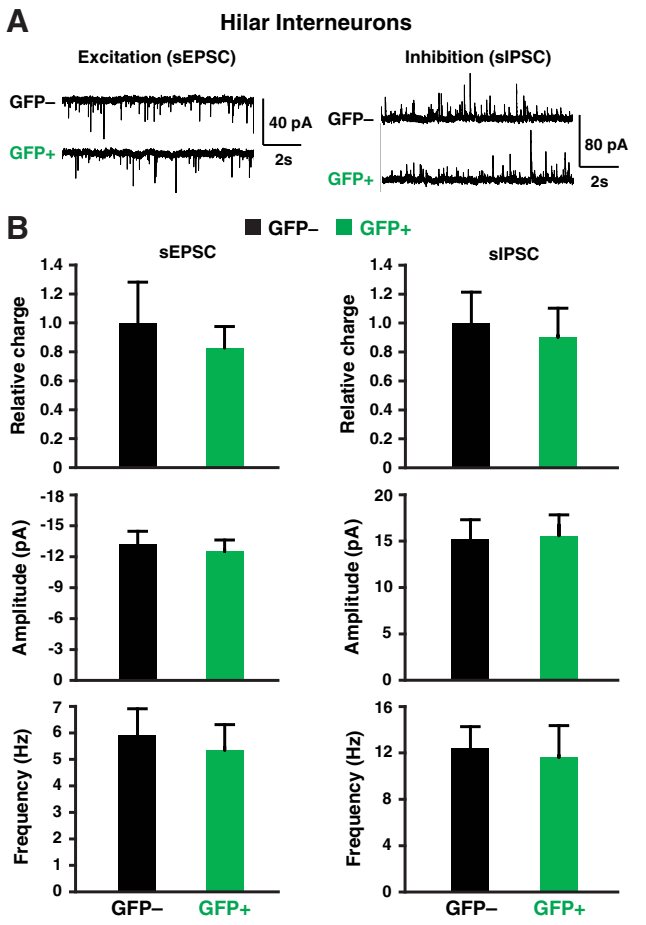

Figure 10. Electrophysiological analyses of transplanted and endogenous cells in acute hippocampal slices from 12-month-old apoE4-KI/hAPP$_{FAD}$ mice at 80–90 DAT. ***A***, Recorded sEPSCs and sIPSCs traces in transplanted GFP+ and endogenous GFP− hilar interneurons. ***B***, Quantification of postsynaptic currents showed similar sEPSC and sIPSC relative charge, amplitude, and frequency in transplanted GFP+ and endogenous GFP− hilar interneurons ($n = 12–18$ cells per group).

to survive and functionally integrate in the brains of AD patients.

Interestingly and importantly, the transplanted MGE cells appear to have a minimal effect on learning and memory in apoE3-KI recipients with normal cognition. We previously reported a threshold number of hilar GABAergic interneurons (~2500–3000) that appeared to distinguish normal versus impaired learning and memory in female apoE4-KI mice at 16 months of age (Andrews-Zwilling et al., 2010; Leung et al., 2012). At this age, all female apoE3-KI mice had >3000 hilar GABAergic interneurons (with a wide range of 3000–5200 interneurons), whereas some of the female apoE4-KI mice had <3000 interneurons and had greater learning deficits. Thus, adding ~1000 hilar interneurons by MGE cell transplantation significantly improved learning and memory performance in female apoE4-KI mice. Since there was no correlation between hilar GABAergic interneuron numbers and normal learning and memory performance in apoE3-KI mice with a wide range of hilar interneurons (3000–5200; Andrews-Zwilling et al., 2010; Leung et al., 2012), it is not surprising that hilar MGE cell transplantation, which adds ~1000 interneurons, has a minimal effect on normal learning and memory in apoE3-KI mice.

To date, all efforts to develop therapies that target specific AD-related pathways have failed in human trials of late-stage AD (Huang and Mucke, 2012). As a result, an emerging consensus in the field is that treatment of moderate-to-advanced AD patients with current drugs comes too late, probably due to neuronal loss in the hippocampus (Huang and Mucke, 2012). In this regard, cell replacement therapies, such as using human embryonic stem cell-derived or induced pluripotent stem cell-derived MGE-like cells (Liu et al., 2013), hold a potential for the treatment of patients with moderate-to-advanced AD. A key aspect of hilar GABAergic interneurons is that one such inhibitory neuron connects to and thus influences >1500 excitatory granule neurons in the dentate gyrus (Morgan et al., 2007). This suggests that even if a small number of the transplanted therapeutic cells survive and functionally integrate, they could make a significant functional improvement in the dentate gyrus and thus in learning and memory. Our findings that ~1000 functionally integrated transplanted GABAergic interneurons are sufficient to rescue apoE4- and Aβ-induced learning and memory deficits in two widely used AD-related mouse models strongly support this notion.

References

Alvarez Dolado M, Broccoli V (2011) GABAergic neuronal precursor grafting: implications in brain regeneration and plasticity. Neural Plast 2011: 384216. CrossRef Medline

Alvarez-Dolado M, Calcagnotto ME, Karkar KM, Southwell DG, Jones-Davis DM, Estrada RC, Rubenstein JL, Alvarez-Buylla A, Baraban SC (2006) Cortical inhibition modified by embryonic neural precursors grafted into the postnatal brain. J Neurosci 26:7380–7389. CrossRef Medline

Anderson S, Mione M, Yun K, Rubenstein JL (1999) Differential origins of neocortical projection and local circuit neurons: role of Dlx genes in neocortical interneuronogenesis. Cereb Cortex 9:646–654. CrossRef Medline

Andrews-Zwilling Y, Bien-Ly N, Xu Q, Li G, Bernardo A, Yoon SY, Zwilling D, Yan TX, Chen L, Huang Y (2010) Apolipoprotein E4 causes age- and tau-dependent impairment of GABAergic interneurons, leading to learning and memory deficits in mice. J Neurosci 30:13707–13717. CrossRef Medline

Andrews-Zwilling Y, Gillespie AK, Kravitz AV, Nelson AB, Devidze N, Lo I, Yoon SY, Bien-Ly N, Ring K, Zwilling D, Potter GB, Rubenstein JL, Kreitzer AC, Huang Y (2012) Hilar GABAergic interneuron activity controls spatial learning and memory retrieval. PLoS One 7:e40555. CrossRef Medline

Bakker A, Krauss GL, Albert MS, Speck CL, Jones LR, Stark CE, Yassa MA, Bassett SS, Shelton AL, Gallagher M (2012) Reduction of hippocampal hyperactivity improves cognition in amnestic mild cognitive impairment. Neuron 74:467–474. CrossRef Medline

Baraban SC, Southwell DG, Estrada RC, Jones DL, Sebe JY, Alfaro-Cervello C, García-Verdugo JM, Rubenstein JL, Alvarez-Buylla A (2009) Reduction of seizures by transplantation of cortical GABAergic interneuron precursors into Kv1.1 mutant mice. Proc Natl Acad Sci U S A 106:15472–15477. CrossRef Medline

Bareggi SR, Franceschi M, Bonini L, Zecca L, Smirne S (1982) Decreased CSF concentrations of homovanillic acid and γ-aminobutyric acid in Alzheimer's disease. Age- or disease-related modifications? Arch Neurol 39:709–712. CrossRef Medline

Bertram L, Lill CM, Tanzi RE (2010) The genetics of Alzheimer's disease: back to the future. Neuron 68:270–281. CrossRef Medline

Bien-Ly N, Andrews-Zwilling Y, Xu Q, Bernardo A, Wang C, Huang Y (2011) C-terminal-truncated apolipoprotein (apo) E4 inefficiently clears amyloid-β (Aβ) and acts in concert with Aβ to elicit neuronal and behavioral deficits in mice. Proc Natl Acad Sci U S A 108:4236–4241. CrossRef Medline

Bien-Ly N, Gillespie AK, Walker D, Yoon SY, Huang Y (2012) Reducing human apolipoprotein E levels attenuates age-dependent Aβ accumulation in mutant human amyloid precursor protein transgenic mice. J Neurosci 32:4803–4811. CrossRef Medline

Bráz JM, Sharif-Naeini R, Vogt D, Kriegstein A, Alvarez-Buylla A, Rubenstein JL, Basbaum AI (2012) Foregrain GABAergic neuron precursors integrate into adult spinal cord and reduce injury-induced neuropathic pain. Neuron 74:663–675. CrossRef Medline

Calcagnotto ME, Zipancic I, Piquer-Gil M, Mello LE, Alvarez-Dolado M

(2010) Grafting of GABAergic precursors rescues deficits in hippocampal inhibition. Epilepsia 51 [Suppl 3]:66–70. CrossRef Medline

Campion D, Dumanchin C, Hannequin D, Dubois B, Belliard S, Puel M, Thomas-Anterion C, Michon A, Martin C, Charbonnier F, Raux G, Camuzat A, Penet C, Mesnage V, Martinez M, Clerget-Darpoux F, Brice A, Frebourg T (1999) Early-onset autosomal dominant Alzheimer disease: prevalence, genetic heterogeneity, and mutation spectrum. Am J Hum Genet 65:664–670. CrossRef Medline

Cui Y, Costa RM, Murphy GG, Elgersma Y, Zhu Y, Gutmann DH, Parada LF, Mody I, Silva AJ (2008) Neurofibromin regulation of ERK signaling modulates GABA release and learning. Cell 135:549–560. CrossRef Medline

Davies P, Katzman R, Terry RD (1980) Reduced somatostatin-like immunoreactivity in cerebral cortex from cases of Alzheimer disease and Alzheimer senile dementia. Nature 288:279–280. CrossRef Medline

Dennis NA, Browndyke JN, Stokes J, Need A, Burke JR, Welsh-Bohmer KA, Cabeza R (2010) Temporal lobe functional activity and connectivity in young adult APOE e4 carriers. Alzheimers Dement 6:303–311. CrossRef Medline

Filippini N, MacIntosh BJ, Hough MG, Goodwin GM, Frisoni GB, Smith SM, Matthews PM, Beckmann CF, Mackay CE (2009) Distinct patterns of brain activity in young carriers of the APOE-ε4 allele. Proc Natl Acad Sci U S A 106:7209–7214. CrossRef Medline

Grouselle D, Winsky-Sommerer R, David JP, Delacourte A, Dournaud P, Epelbaum J (1998) Loss of somatostatin-like immunoreactivity in the frontal cortex of Alzheimer patients carrying the apolipoprotein epsilon 4 allele. Neurosci Lett 255:21–24. CrossRef Medline

Hamanaka H, Katoh-Fukui Y, Suzuki K, Kobayashi M, Suzuki R, Motegi Y, Nakahara Y, Takeshita A, Kawai M, Ishiguro K, Yokoyama M, Fujita SC (2000) Altered cholesterol metabolism in human apolipoprotein E4 knock-in mice. Hum Mol Genet 9:353–361. CrossRef Medline

Hardy J, Cowburn R, Barton A, Reynolds G, Dodd P, Wester P, O"Carroll AM, Lofdahl E, Winblad B (1987) A disorder of cortical GABAergic innervation in Alzheimer's disease. Neurosci Lett 73:192–196. CrossRef Medline

Huang Y, Mucke L (2012) Alzheimer mechanisms and therapeutic strategies. Cell 148:1204–1222. CrossRef Medline

Hunt RF, Girskis KM, Rubenstein JL, Alvarez-Buylla A, Baraban SC (2013) GABA progenitors grafted into the adult epileptic brain control seizures and abnormal behavior. Nat Neurosci 16:692–697. CrossRef Medline

Leung L, Andrews-Zwilling Y, Yoon SY, Jain S, Ring K, Dai J, Wang MM, Tong L, Walker D, Huang Y (2012) Apolipoprotein E4 causes age- and sex-dependent impairments of hilar GABAergic interneurons and learning and memory deficits in mice. PLoS One 7:e53569. CrossRef Medline

Li G, Bien-Ly N, Andrews-Zwilling Y, Xu Q, Bernardo A, Ring K, Halabisky B, Deng C, Mahley RW, Huang Y (2009) GABAergic interneuron dysfunction impairs hippocampal neurogenesis in adult apolipoprotein E4 knockin mice. Cell Stem Cell 5:634–645. CrossRef Medline

Liu Y, Weick JP, Liu H, Krencik R, Zhang X, Ma L, Zhou GM, Ayala M, Zhang SC (2013) Medial ganglionic eminence-like cells derived from human embryonic stem cells correct learning and memory deficits. Nat Biotechnol 31:440–447. CrossRef Medline

Martínez-Cerdeño V, Noctor SC, Espinosa A, Ariza J, Parker P, Orasji S, Daadi MM, Bankiewicz K, Alvarez-Buylla A, Kriegstein AR (2010) Embryonic MGE precursor cells grafted into adult rat striatum integrate and ameliorate motor symptoms in 6-OHDA-lesioned rats. Cell Stem Cell 6:238–250. CrossRef Medline

Morellini F, Sivukhina E, Stoenica L, Oulianova E, Bukalo O, Jakovcevski I, Dityatev A, Irintchev A, Schachner M (2010) Improved reversal learning and working memory and enhanced reactivity to novelty in mice with enhanced GABAergic innervation in the dentate gyrus. Cereb Cortex 20:2712–2727. CrossRef Medline

Morgan RJ, Santhakumar V, Soltesz I (2007) Modeling the dentate gyrus. Prog Brain Res 163:639–658. CrossRef Medline

Mucke L, Masliah E, Yu GQ, Mallory M, Rockenstein EM, Tatsuno G, Hu K, Kholodenko D, Johnson-Wood K, McConlogue L (2000) High-level neuronal expression of Ab_{1-42} in wild-type human amyloid protein precursor transgenic mice: synaptotoxicity without plaque formation. J Neurosci 20:4050–4058. Medline

Palop JJ, Mucke L (2010) Amyloid-β-induced neuronal dysfunction in Alzheimer's disease: from synapses toward neural networks. Nat Neurosci 13:812–818. CrossRef Medline

Palop JJ, Chin J, Roberson ED, Wang J, Thwin MT, Bien-Ly N, Yoo J, Ho KO, Yu GQ, Kreitzer A, Finkbeiner S, Noebels JL, Mucke L (2007) Aberrant excitatory neuronal activity and compensatory remodeling of inhibitory hippocampal circuits in moue models of Alzheimer's disease. Neuron 55:697–711. CrossRef Medline

Seidl R, Cairns N, Singewald N, Kaehler ST, Lubec G (2001) Differences between GABA levels in Alzheimer's disease and Down syndrome with Alzheimer-like neuropathology. Naunyn Schmiedebergs Arch Pharmacol 363:139–145. CrossRef Medline

Southwell DG, Froemke RC, Alvarez-Buylla A, Stryker MP, Gandhi SP (2010) Cortical plasticity induced by inhibitory neuron transplantation. Science 327:1145–1148. CrossRef Medline

Tanaka DH, Toriumi K, Kubo K, Nabeshima T, Nakajima K (2011) GABAergic precursor transplantation into the prefrontal cortex prevents phencyclidine-induced cognitive deficits. J Neurosci 31:14116–14125. CrossRef Medline

Tricoire L, Pelkey KA, Erkkila BE, Jeffries BW, Yuan X, McBain CJ (2011) A blueprint for the spatiotemporal origins of mouse hippocampal interneuron diversity. J Neurosci 31:10948–10970. CrossRef Medline

Verret L, Mann EO, Hang GB, Barth AM, Cobos I, Ho K, Devidze N, Masliah E, Kreitzer AC, Mody I, Mucke L, Palop JJ (2012) Inhibitory interneuron deficit links altered network activity and cognitive dysfunction in Alzheimer model. Cell 149:708–721. CrossRef Medline

Wichterle H, Garcia-Verdugo JM, Herrera DG, Alvarez-Buylla A (1999) Young neurons from medial ganglionic eminence disperse in adult and embryonic brain. Nat Neurosci 2:461–466. CrossRef Medline

Yassa MA, Stark SM, Bakker A, Albert MS, Gallagher M, Stark CE (2010) High-resolution structural and functional MRI of hippocampal CA3 and dentate gyrus in patients with amnestic mild cognitive impairment. Neuroimage 51:1242–1252. CrossRef Medline

Zhao S, Ting JT, Atallah HE, Qiu L, Tan J, Gloss B, Augustine GJ, Deisseroth K, Luo M, Graybiel AM, Feng G (2011) Cell type-specific channelrhodopsin-2 transgenic mice for optogenetic dissection of neural circuitry function. Nat Methods 8:745–752. CrossRef Medline

Zimmer R, Teelken AW, Trieling WB, Weber W, Weihmayr T, Lauter H (1984) γ-aminobutyric acid and homovanillic acid concentration in the CSF of patients with senile dementia of Alzheimer's type. Arch Neurol 41:602–604. CrossRef Medline

Zipancic I, Calcagnotto ME, Piquer-Gil M, Mello LE, Alvarez-Dolado M (2010) Transplant of GABAergic precursors restores hippocampal inhibitory function in a mouse model of seizure susceptibility. Cell Transplant 19:549–564. CrossRef Medline